Research Article

Internode Distance-Based Redundancy Reliable Transport in Underwater Sensor Networks

Bin Liu,[1] Hongyang Chen,[2] Xianfu Lei,[3] Fengyuan Ren,[4] and Kaoru Sezaki[2]

[1] *Computer Science Department, University of Southern California, Los Angeles, CA 90089, USA*
[2] *Institute of Industrial Science, The University of Tokyo, Tokyo, Japan*
[3] *Institute of Mobile Communications, Southwest Jiaotong University, Chengdu, China*
[4] *Department of Computer Science and Technology, Tsinghua University, Beijing, China*

Correspondence should be addressed to Hongyang Chen, hongyang@mcl.iis.u-tokyo.ac.jp

Underwater communication is a very challenging topic. Protocols used in terrestrial sensor networks cannot be directly applied in the underwater world. High-bit error rate and large propagation delay make the design of transport protocols especially awkward. ARQ-based reliable transport schemes are not appropriate in underwater environments due to large propagation delay, low communication bandwidth, and high error probability. Thus, we focus on redundancy-based transport schemes in this paper. We first investigate three schemes that employ redundancy mechanisms at the bit and/or packet level to increase the reliability in a direct link scenario. Then, we show that the broadcast property of the underwater channel allows us to extend those schemes to a case with node cooperative communication. Based on our analysis, an adaptive redundancy transport protocol (ARRTP) for underwater sensor networks is proposed. We suggest an architecture for implementation. For two kinds of topologies, namely, regular and random, we show that ARRTP presents a better transmission success probability and energy efficiency tradeoff for single- and multihop transmissions. We also offer an integrated case study to show that ARRTP is not only supplying reliability but also has some positive effect in guiding the deployment of underwater sensor nodes.

1. Introduction

Understanding the key mechanisms of the oceans is crucial for the knowledge of the Earth's climate and atmosphere. Over the past few years, there has been a relentless effort to investigate the abyssal plain in the oceans. This interest is highly motivated by various applications, such as scientific exploration, commercial exploitation, oceanographic data collection, pollution monitoring, tactical surveillance, and coastline protection. Underwater Sensor Networks (UWSNs) are proving to be a promising technique for these applications [1, 2].

As in terrestrial wireless sensor networks, reliable data transport is one of the basic elements in UWSNs because mission critical applications need its support. The problem of reliable data delivery in multihop wireless networks is by itself not new and has been addressed by many existing works in the context of terrestrial wireless networks [3, 4].

However, these approaches cannot be directly applied to UWSNs because radio communication in terrestrial wireless networks is replaced with acoustic communication in aquatic environments.

There are several significant distinctions between the terrestrial radio-based channel and the underwater acoustic channel. One is that the signal propagation speed in the underwater acoustic channel is around $1.5 \cdot 10^3$ m/s, which is five orders of magnitude lower than the radio propagation speed ($3 \cdot 10^8$ m/s). Secondly, the available bandwidth of the underwater acoustic channel is limited and strongly depends upon both transmission range and frequency (e.g., the longer the communication distance, the lower the available bandwidth of the underwater acoustic channel); most commercial acoustic modems operate below 30 kHz. In addition, the underwater acoustic channel is affected by many possible factors, such as path loss, noise, multipath and Doppler spread. The path loss is caused by spreading and absorption.

The noise comes from various sources such as the movement of water, rain and wind, seismic and volcanic activities or biological phenomena, which are obviously different compared to their counterpart in terrestrial environments. In shallow waters, the signal reflection from the surface and seabed creates multipaths whereas in deep waters, this may occur due to topographic sources like hills, cliffs, or hollows. Phase and amplitude fluctuations caused by relatively large motion-induced Doppler spreads also lead to a high bit-error probability relative to most radio channels.

In short, the underwater acoustic channel features large propagation delays, limited available bandwidth, and high error probability. All these features pose challenges for reliable data transport in UWSNs.

Broadly speaking, there are two types of approaches for reliable data transport, namely, *endtoend* and *hopbyhop*. Many studies have shown that the end-to-end approach is infeasible for terrestrial sensor networks [3–5]. This conclusion still holds in underwater sensor networks and is additionally justified by the large propagation delay and the high error probability. The very large end-to-end delay introduces difficulties for the two ends to manage data transmission timely, while the high channel error probability makes the success probability of end-to-end data transport rather low which results in too many retransmissions for a success packet delivery. Thus, the *hop-by-hop* approaches are more appropriate for UWSNs.

Additionally, the hop-by-hop reliability can be guaranteed by providing either *Retransmission* or *Redundancy*. Retransmission [6] is the most common reliable transport scheme which allows a receiver to recover from retransmitting error packets. Although it works well in terrestrial networks, such scheme-like automatic repeat request (ARQ) mechanisms are not appropriate in the underwater world mainly because of the propagation delay but also because of the energy consumption.

(i) The *large propagation delay* leads to a large hop-by-hop RTT. Thus, if the sender uses feedbacks from the receiver to pace its sending rate, it will wait a long period of time to ensure a successful transmission, which makes the utilization of communication channels very low.

(ii) The *high error probability* may cause more packet losses in the UWSNs than in the terrestrial sensor networks. And the *limited available bandwidth* will be further wasted in the case of lost feedback. If positive feedback transmissions are lost, not only will the bandwidth resources be wasted, but also some successfully received packets will be retransmitted by the sender, causing more energy consumption. Similarly, if negative feedback transmissions are lost, the successive retransmitted NACKs will consume the valuable bandwidth as well as cost extra energy and increase the communication delay.

Besides feedback-based *retransmission* mechanisms, *redundancy* transmission is another effective approach to achieve high reliability. Redundancy transmission can be implemented at the bit level [7] and at the packet level [8], which correspond to bit level forward error correction (FEC) and packet level erasure coding, respectively. Bit level FEC is a typical bit error detection and correction mechanism, and there have been many mature algorithms, such as BCH codes and convolutional codes. Erasure coding at the packet level works as follows. M original packets are encoded into $M + R$ packets for reliable transmission, so as to recover M original packets if receiving at least $(1 + \varepsilon)M$ out of the $M + R$ encoded data packets. Here, ε is a small constant and varies depending on concrete algorithms, such as Reed-Solomon codes or Tornado codes. Compared with retransmission-based reliable transport schemes, redundancy-based schemes can avoid the inconveniences caused by feedback. However, in the case of sensor nodes, for both kinds of redundancy, error control parities consume valuable transceiver energy which must be taken into account. The encoding/decoding energy also needs to be incorporated.

From the above analysis, we believe that *redundancy-based hop-by-hop reliable transport mechanisms* are preferred in underwater environment and we will investigate them in this paper. This paper begins with a brief review of the literature on reliable transport protocols in UWSNs. Then, in Section 3, we define in more details the characteristics of acoustic channels and give its mathematical model. Applying BCH and/or Reed-Solomon codes, three reliable transport schemes are proposed and analyzed in two different scenarios: with and without cooperation (Sections 4 and 5) between nodes. Based on these analyses, Section 6 presents an integrated adaptive redundancy reliable transport protocol (ARRTP) and its implementation framework. Simulations are conducted to demonstrate the benefits of our proposed protocol in Section 7. We also propose an initial idea about how to apply ARRTP to topology management in Section 8. Finally, we conclude our work in Section 9.

2. Related Work

Nearly all of the reliable transport protocols for terrestrial sensor networks (such as PSFQ [4] and RMST [3]) are based on the ARQ mechanism and thus, not applicable to underwater sensor networks. And so far, reliable transport protocols for underwater sensor networks have not been addressed except recently [9, 10].

In [9], the authors introduce a per-hop hybrid implicit/explicit acknowledgement scheme for stop and wait ARQ in a multi-hop acoustic channel. In this scheme, when a relay node receives a packet, it sends an acknowledgement message only when its previous data transmission has been already acknowledged. The acknowledgement can be implicit with the data packet itself or explicit with an acknowledgement message. Unfortunately, both mechanisms have a high time-out. They demonstrate that their protocol has a better latency and energy efficiency than the traditional schemes. However, the latency remains high and when the explicit acknowledgement is used, it increases the energy expenditure.

In [10], the authors propose a segmented data reliable transport protocol called SDRT. SDRT is a hybrid of FEC and ARQ. It uses erasure codes (simple variant of Tornado codes) to send data block by block and hop by hop. Basically, the source encodes and sends a data block to the next node. The intermediate node decodes, reconstructs, and re-encodes the data block. Then it forwards it to the next node. The sender continues to pump encoded packets into the channel until it receives a positive acknowledgement message from its next node. SDRT reduces the total number of transmitted packets, improves channel utilization, and simplifies protocol management. On the other hand, its main drawback comes from the utilization of ARQ packets. Indeed, SDRT keeps sending packets until it receives a positive feedback which obviously wastes energy. Furthermore, if a node suddenly stops relaying, the sender will hardly detect it, which leads to an increased communication cost.

3. Characteristics of Underwater Channels

We have previously stated that underwater communication diverges from the terrestrial wireless one. In this section, we mathematically characterize the features of underwater acoustic channels and present its analytical model for the convenience of discussion in the rest of this paper.

Since the acoustic signal is prone to multipath propagation, the underwater acoustic channel is usually modeled as a Rayleigh fading one [11]. We assume that the binary phase shift keying (BPSK) is used to calculate the average bit error rate (BER), and γ_s and γ_b denote the signal-to-noise ratio (SNR) per symbol and per bit, respectively. In BPSK, one symbol error corresponds to exactly one uncoded bit error, that is, $\gamma_s = \gamma_b$. Let

$$\overline{\gamma}_s = 10^{\gamma_s/10} = 10^{\gamma_b/10}. \tag{1}$$

We can get the average BER using BPSK in an underwater Rayleigh fading channel [12] from.

$$\text{BER}(\gamma_b) = \frac{1}{2}\left(1 - \sqrt{\frac{\overline{\gamma}_s}{1 + \overline{\gamma}_s}}\right). \tag{2}$$

The passive sonar equation [13] describes the SNR per bit of a signal from a source at the receiver side:

$$\gamma_b = \text{SL} - \text{TL} - \text{NL} + \text{DI}, \tag{3}$$

where SL denotes the source level which determines the transmission power, TL denotes the transmission loss, NL denotes the noise level, and DI denotes the directivity index (all quantities are in dB). In the following, we consider omnidirectional hydrophones, which implies that the diversity index is 0.

The transmission loss over a distance d in km for a cylindrically spread signal of frequency f in kHz is given by

$$\text{TL}(d, f) = 10 \log_{10}d + \alpha(f)d + 30, \tag{4}$$

where $\alpha(f)$ is the absorption coefficient.

We use the Thorp's formula [13, 14] for the absorption coefficient in dB/km:

$$\alpha(f) = 0.11\frac{f^2}{1 + f^2} + 44\frac{f^2}{4100 + f^2} + 2.75 \cdot 10^{-4}f^2 + 0.003. \tag{5}$$

The noise is composed of four components: turbulence, shipping, waves, and thermal noise. The empirical formulae are given in [15]. For simplicity, we employ a useful approximation presented in [16], namely.

$$\text{NL}(f) = 50 - 18 \log_{10}f. \tag{6}$$

From (3), (4), and (6), we obtain.

$$\gamma_b = \text{SL} - 10 \log_{10}d - \alpha(f)d \cdot 10^{-3} - 50 + 18 \log_{10}f. \tag{7}$$

We have seen in (2) that the SNR per bit γ_b directly determines the BER. In order to increase the transmission reliability, we can get its maximum value by computing the derivative $\partial\gamma_b/\partial f$:

$$\frac{\partial\gamma_b}{\partial f} = \frac{18}{f \ln 10} - fd\left[\frac{2.2 \cdot 10^{-4}}{(1 + f^2)^2} + \frac{360.8}{(4100 + f^2)^2} + 5.5 \cdot 10^{-7}\right]. \tag{8}$$

In UWSNs, the internode distance d is usually in the range of 0.1 to 100 km. (Unless otherwise specified, the term "the internode distance" means "the horizontal internode distance" in this paper.) Thus, for for all $d \in [0.1, 100]$:

$$\lim_{f \to 0} \frac{\partial\gamma_b}{\partial f} = +\infty, \qquad \lim_{f \to +\infty} \frac{\partial\gamma_b}{\partial f} = -\infty. \tag{9}$$

In other words, for $d \in [0.1, 100]$, there exists one frequency where the SNR per bit γ_b is maximum (some examples are shown in Figure 1(a)). This frequency is denoted by $f^*(d)$, which is the optimal transmission frequency and plotted in Figure 1(b). When the transmitter works on this frequency, the bit error rate is only related to the distance (d) between the sender and the receiver. Therefore, BER(γ_b) in (2) can be replaced with the notation BER(d).

The sound intensity of a source is related to a reference intensity and is given by

$$I_t = 10^{\text{SL/10}}I_{\text{ref}}, \tag{10}$$

where $I_{\text{ref}} = p^2/2\rho c$, with p being the effective sound pressure, ρ the density of sea water, and c the propagation velocity of the sound wave in sea water. The speed of sound varies with the pressure, temperature, and salinity and thus depends on the environment. The pressure depends on the depth as well. For simplicity, we assume a constant speed of $c = 1500$ m/s. Thus, we take $I_{\text{ref}} = 0.67 \cdot 10^{-18}$ W/m^2.

In the case of cylindrical spreading, the power P_t required to achieve intensity I_t at 1 m from the source in the direction of the receiver is expressed as

$$P_t = 2\pi zI_t, \tag{11}$$

where P_t in watts and z is the depth in meters.

(a) γ_b in 150 dB SL (source level)
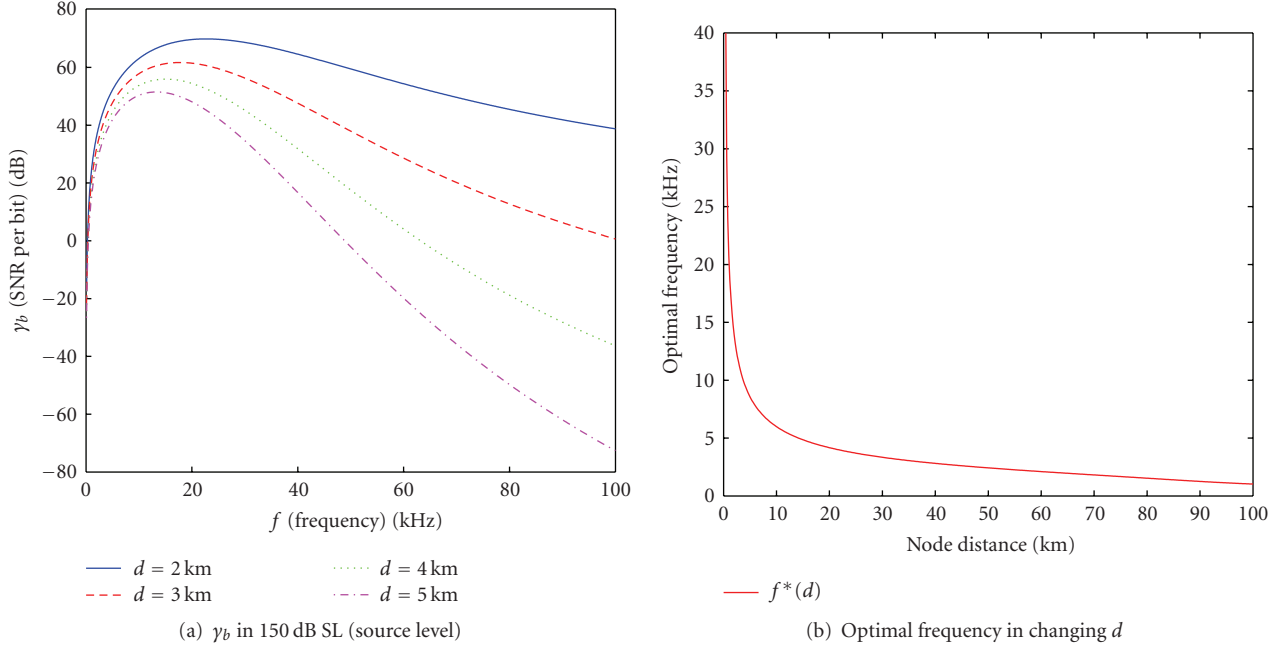
(b) Optimal frequency in changing d

FIGURE 1: Optimal frequency.

For commercial hydrophones [17], the energy needed to receive a packet is typically around one fifth of the transmitted energy. In addition, we assume that if the frequency is $f^*(d)$ kHz, the available bit rate is $r = f^*(d)$ kb/s. Therefore, for transmitting and receiving an l bits packet, the required energy E_t and E_r are.

$$E_t(l) = P_t \frac{l}{r} 10^{-3}, \tag{12}$$

$$E_r(l) = \frac{1}{5} E_t(l). \tag{13}$$

4. Basic Redundancy Schemes and Their Performances

To determine the proper redundancy reliable transport mechanisms, we firstly investigate three different implementations as depicted in Figure 2. The first implementation encodes data packets with bit-level FEC; whereas the second one uses packet-level erasure coding. Finally, the third one is a hybrid solution that integrates packet-level erasure coding and bit level FEC.

For the bit-level FEC, there are mainly two kinds of codes: BCH codes and convolutional codes. We consider the former type not only because BCH codes are more efficient decoding algorithms but also consider that the energy efficiency is rather low when apply convolutional codes to sensor networks [18]. As for BCH, we consider the special case of binary BCH codes. For these codes, the following property holds [19]. For all positive integers m and t, there exists a binary BCH code that has a code segment length of $n = 2^m - 1$, of which at most $\phi = mt$ are overhead bits that can reliably correct up to t errors.

For the packet-level erasure coding, the two types of codes are linear codes ($\varepsilon = 0$) and nonlinear codes ($\varepsilon > 0$). Linear codes, such as Reed-Solomon (RS) codes [20], have better error correction capabilities but consume more energy in the encoding/decoding process than nonlinear codes (e.g., Random codes [21] and LT codes [22]). Fortunately, we can use a "look-up table" method to replace some of the complex encoding/decoding calculations when linear codes are employed in sensor nodes with restricted computational resources [5]. So the most common linear codes, RS codes are chosen here. For RS codes, k original data packets can be reconstructed by receiving any k packets out of $k + s$ ones, with s check packets.

Thus, we can refer to the three implementations in Figure 2 as the BCH scheme, the RS scheme, and the RS_BCH scheme, respectively. In this section, we first study the performances of the three schemes in a simple communication scenario between two nodes. Then in Section 5, when additionally utilizing node redundancy and the broadcast property of the underwater channel in large-scale UWSNs, we analyze the three schemes in a cooperative scenario in which a source node can send data to a destination with the help of a third relaying node. The two metrics employed are the success probability of transmitting a block of packets and the expected total energy consumption.

4.1. Success Probability of Transmitting a Block (k) of Packets. Assuming that the transmitter works on the optimal frequency $f^*(d)$, the probability of a successful transmission of a single packet of length l over one hop of distance d is

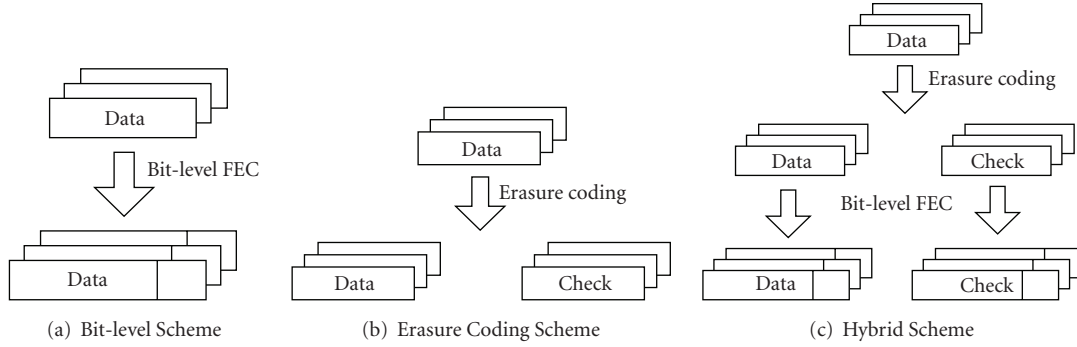$$p(l, d) = (1 - \text{BER}(d))^l. \tag{14}$$

FIGURE 2: Different schemes.

When the BCH scheme is employed, we can obtain the probability of a successful transmission of a single packet of length l which can reliably correct up to t errors over one hop of distance d as

$$p_{\text{BCH}}(l, t, d) = \sum_{i=0}^{t} \binom{l}{i} (1 - \text{BER}(d))^{l-i} \text{BER}^i(d). \qquad (15)$$

As for the two RS-based schemes, since reconstructing k original data packets needs receiving any k packets out of $k + s$ packets, the probability of a successful transmission of k packets is given by.

$$p_{\text{RS}}(k, s, p_s) = \sum_{i=k}^{k+s} \binom{k+s}{i} p_s^i (1 - p_s)^{k+s-i}, \qquad (16)$$

where p_s is the probability of successfully transmitting one packet over one hop.

For the convenience of comparing performances of the three different schemes, we define the probability of successfully transmitting k packets over one hop as p_1, p_2, and p_3 for BCH, RS and RS_BCH schemes, respectively,

$$\begin{aligned} p_1 &= p_{\text{BCH}}^k(l, t, d), \\ p_i &= p_{\text{RS}}(k, s, p_{s,i}), \end{aligned} \qquad (17)$$

for $i = \{2, 3\}$ and $p_{s,i}$ in (17) are defined as follows:

$$\begin{aligned} p_{s,2} &= p(l - \phi, d), \\ p_{s,3} &= p_{\text{BCH}}(l, t, d). \end{aligned} \qquad (18)$$

In (18), because RS schemes do not employ bit-level FEC, we subtract ϕ which is the overhead due to BCH encoding. (Instead of bit-level FEC, cyclic redundancy check (CRC) can be used in the RS scheme. We assume that CRC can detect every possible packet error and neglect the messaging overhead [18].)

4.2. Expected Total Energy Consumption. Energy efficiency is an important performance metric for battery-powered UWSN nodes. In this subsection, we analyze and evaluate energy consumption of the three reliable transport schemes.

For bit-level FEC redundancy schemes, since the BCH encoding process uses a linear-feedback shift register [23], the encoding energy is negligible [24]. On the other hand, BCH code employs an efficient decoding technique based on the *Berlekamp-Massey (BM)* and *Chien's search (CS)* algorithms [7, 25], so the computation complexity of the decoding process merely relates with packet length l. The energy consumption models for these algorithms have been outlined in [25, 26] as follows:

$$E_{\text{dec}}(l, t) = (2lt + 2t^2)(E_{\text{add}} + E_{\text{mul}}), \qquad (19)$$

where E_{mul} and E_{add} are the energy of the multiplication and addition processes, respectively, in the Galois field $GF(2^m)$, with $m = \lfloor \log_2 n + 1 \rfloor$ being used in BCH. In [18], the typical value of E_{mul} and E_{add} is fixed at $E_{\text{mul}} = 3.7 \cdot 10^{-14} \, \text{m}^3$ and $E_{\text{add}} = 3.3 \cdot 10^{-14} \, \text{m}$, respectively.

As early mentioned, we use a "look-up table" method to implement RS, codes as the packet-level erasure coding. In [5], finite fields operations and look-up tables are suggested to avoid heavy operations, such as vector arithmetic and matrix inversions in the encoding and decoding processes of RS codes. In this paper, we assume that the packet number of a block is relatively small, that is, no more than 8 packets per block, which is suitable for "look-up table" approach. Thus, the energy spent on encoding and decoding is negligible when we consider the energy spent on sending and receiving the redundancy check packets [5].

Given the preceding assumptions, the energy consumption of each scheme for successful transmission of k data packets is

$$\begin{aligned} E_1 &= k(E_{\text{dec}}(l, t) + E_t(l) + E_r(l)), \\ E_2 &= (k + s)(E_t(l) + E_r(l)), \\ E_3 &= (k + s)(E_{\text{dec}}(l, t) + E_t(l) + E_r(l)), \end{aligned} \qquad (20)$$

where $E_t(l)$ and $E_r(l)$ come from (12) and (13).

Finally, the expected total energy consumption of *scheme i* for k data packets over n hops is given by

$$E_{i,\text{tot}}(n) = nE_i p_i^n + \sum_{j=0}^{n-1}(j+1)E_i p_i^j(1-p_i)$$

$$= E_i \frac{1-p_i^n}{1-p_i}. \qquad (21)$$

4.3. Numerical Results. Although we have presented the models for both single- and multihop communications, we only present the numerical results for one-hop transmission in this subsection. This will guide our protocol design in Section 6.

Assume that the depth is 10 m and we use BCH with $m = 10$ and $t = 2$. Therefore, the packet length is $l = 1023$ bits and the overhead $\phi = 20$ bits. Transmissions are based on block and each block consists of 4 data packets. According to the experimental results of [5], the added redundancy should not exceed 50% of the block size. Thus, for our 4 data packets per block, we set the redundancy check packet number to 1 or 2. Four concrete schemes, that is, BCH scheme, RS scheme with two redundancy packets, and RS_BCH scheme with one or two redundancy packets, are discussed here and referred as BCH, RS (2), RS_BCH (1), and RS_BCH (2), respectively.

In this paper, we define that a scheme is reliable if it achieves a hop-by-hop successful transmission probability greater than or equal to 99% for a block of packets. In order to do this, the source level (transmission power level) is set to 131 dB to guarantee that in one hop transmission, for any node distance within [0.1, 100] km, there is at least one scheme that can achieve a success probability above 99%.

The success probability and the expected energy consumption of the four schemes for the hop-by-hop transmission case are plotted in Figures 3(a) and 3(b). The vertical dashed lines represent the distance when a scheme has its probability below the threshold of 99%. Looking at Figures 3(a) and 3(b), we conjecture that for hop-by-hop transmissions, we should use BCH up to the second vertical dashed line, that is, a distance of 62 km, because when the distance is below 62 km, all of the schemes except for RS (2) can achieve not less than 99% probability, while BCH consumes the least energy. RS_BCH (1) should be used between the second and third vertical lines (86 km) because its energy consumption is lower than RS_BCH (2)'s. For the next case, RS_BCH (2) is the most recommendable. Note that RS (2) cannot be used because its energy is too high and its reliability is rather low compared with the other three schemes. We also find that the energy consumption of RS (2) is slightly lower than that of the RS_BCH (2), and this is because we use only a 20-bit overhead in BCH which is rather small compared with the 1023-bit packet length.

5. Redundancy Schemes and Their Performances in Cooperative Scenarios

In dense underwater sensor networks, in addition to bit- and packet-level redundancies, we may also use node-level redundancy, that is, applying cooperative relay to UWSNs. In this section, we analyze the influence of introducing node-level redundancy. We study the case of cooperation between nodes within the scenario depicted in Figure 4 [27, 28]. In this scenario, the source node S wants to send packets to the destination node D. S broadcasts packets to nodes D and R. The relay node R forwards the packets to D and, therefore, provides redundancy.

To simplify the analysis, let $d'' = d'$. Without any forward correction code, we distinguish four cases of a successful transmission of a packet of length l. The following two equations give the total probability of success and the expected energy consumption

$$p_s(l,d,d') = p(l,d) + (1-p(l,d))p^2(l,d')$$

$$E_s(l,d,d') = (E_t(l) + 2E_r(l))p(l,d)(1-p(l,d'))$$
$$+ (2E_t(l) + 3E_r(l))$$
$$\times (p(l,d)p(l,d') + (1-p(l,d))p^2(l,d')). \qquad (22)$$

On the other hand, there are only two cases of failure and the total probability of failure is

$$p_f(l,d,d') = (1-p(l,d))(1-p^2(l,d')). \qquad (23)$$

The expected energy consumption of a failed transmission is given by

$$E_f(l,d,d') = (E_t(l) + 2E_r(l))(1-p(l,d))$$
$$\times (1-p(l,d')) + (2E_t(l) + 3E_r(l)) \qquad (24)$$
$$\times (1-p(l,d))p(l,d')(1-p(l,d')).$$

When we use BCH, we can obtain $p_{s,\text{BCH}}(l,t,d,d')$, $p_{f,\text{BCH}}(l,t,d,d')$, $E_{s,\text{BCH}}(l,t,d,d')$, and $E_{f,\text{BCH}}(l,t,d,d')$ by replacing $p(l,d)$ with $p_{\text{BCH}}(l,t,d)$ in (22)–(24).

With blocks of k packets, we have the probability of success, and energy consumption for successful and failed transmissions of Scheme 1:

$$p_{\text{cs},1} = p_{s,\text{BCH}}^k(l,t,d,d'),$$

$$E_{\text{cs},1} = kE_{s,\text{BCH}}(l,t,d,d'),$$

$$E_{\text{cf},1} = \sum_{j=0}^{k-1}\left(jE_{s,\text{BCH}}(l,t,d,d') + (k-j)\right. \qquad (25)$$

$$\left. E_{f,\text{BCH}}(l,t,d,d')\right)p_{s,1}^j(1-p_{s,1})^{(k-j)}.$$

Schemes $i = \{2,3\}$ with erasure coding use (16) for defining the probability of success $p_{\text{cs},i}$:

$$p_{\text{cs},i} = p_{\text{RS}}(k,s,p_{\text{cs}-i}), \qquad (26)$$

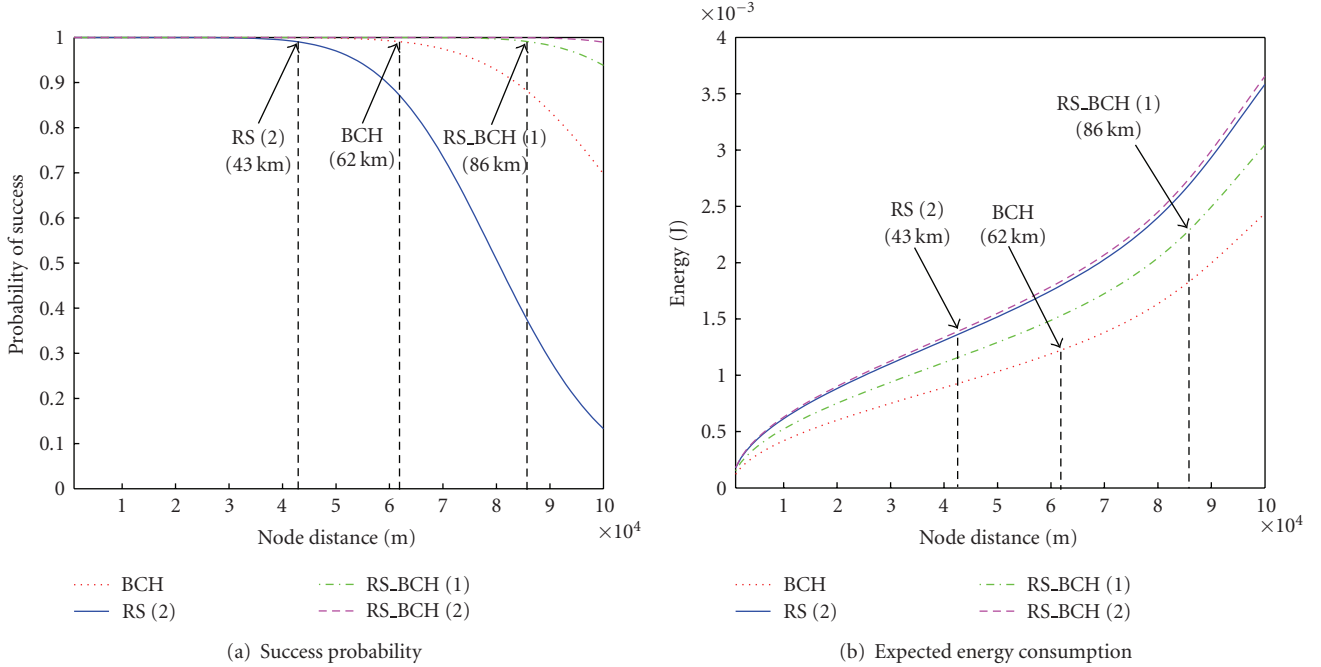where $p_{\text{cs}-i}$ will be defined later.

Figure 3: Analytical results for the noncooperative scenario.

The two equations $E_{cs,i}$ and $E_{cf,i}$ describe the expected energy consumptions for a successful and failed transmission, respectively,

$$E_{cs,i} = \sum_{j=k}^{k+s} \binom{k+s}{j} \left(j E_{cs-i} + (k+s-j) E_{cf-i} \right)$$
$$p_{cs-i}^{j} (1 - p_{cs-i})^{k+s-j}, \tag{27}$$

$$E_{cf,i} = \sum_{j=0}^{k-1} \binom{k+s}{j} \left(j E_{cs-i} + (k+s-j) E_{cf-i} \right)$$
$$p_{cs-i}^{j} (1 - p_{cs-i})^{k+s-j}. \tag{28}$$

p_{cs-i}, E_{cs-i} and E_{cf-i} used in (26)–(28) are

$$p_{cs-2} = p_s(l - \phi, d, d'), \quad E_{cs-2} = E_s(l - \phi, d, d'),$$
$$E_{cf-2} = E_f(l - \phi, d, d'), \quad p_{cs-3} = p_{s,\text{BCH}}(l, t, d, d'), \tag{29}$$
$$E_{cs-3} = E_{s,\text{BCH}}(l, t, d, d'), \quad E_{cf-3} = E_{f,\text{BCH}}(l, t, d, d').$$

If we replicate Figure 4 n times, the total expected energy consumption becomes

$$E_{i,\text{tot}} = n E_{cs} p_{cs}^{n} + \sum_{j=0}^{n-1} (j E_{cs} + E_{cf}) p_{cs}^{j} (1 - p_{cs})$$
$$= \left[\frac{E_{cs} P_{cs}}{1 - p_{cs}} + E_{cf} \right] (1 - p_{cs}^{n}) \tag{30}$$

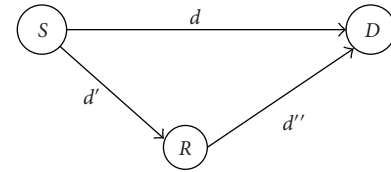for each scheme $i = \{1, 2, 3\}$.

Figure 4: A simple scenario where node S wants to send packets to node D with the help of the relaying node R.

Assuming $d' = d/\sqrt{2}$ in Figure 4, the numerical results for hop-by-hop transmission are shown in Figure 5 by using (26) and (30). The parameters are the same as in the noncooperative scenario except that the required source level SL is lowe; that is, 127 dB is enough to achieve our reliability definition. Then we can get similar principles for cooperative communications; that is, scheme BCH has a lower energy consumption and is applied to the second vertical dashed line at 76 km. Scheme RS_BCH (1) is the best between the second and third lines (92 km). Finally, scheme RS_BCH (2) should be used.

6. Adaptive Redundancy Transport Protocol

6.1. Discussions and Useful Principles. First, by employing the same settings used for the numerical results, we implement several schemes for both hop-by-hop scenarios of Sections 4 and 5. (Inheriting from [29], we extend the wireless package of the *NS-2.31* simulator to simulate the characteristics of the underwater environment. We implement the underwater transmission loss, the transmission and propagation delays, and the physical layer characteristics of underwater receivers
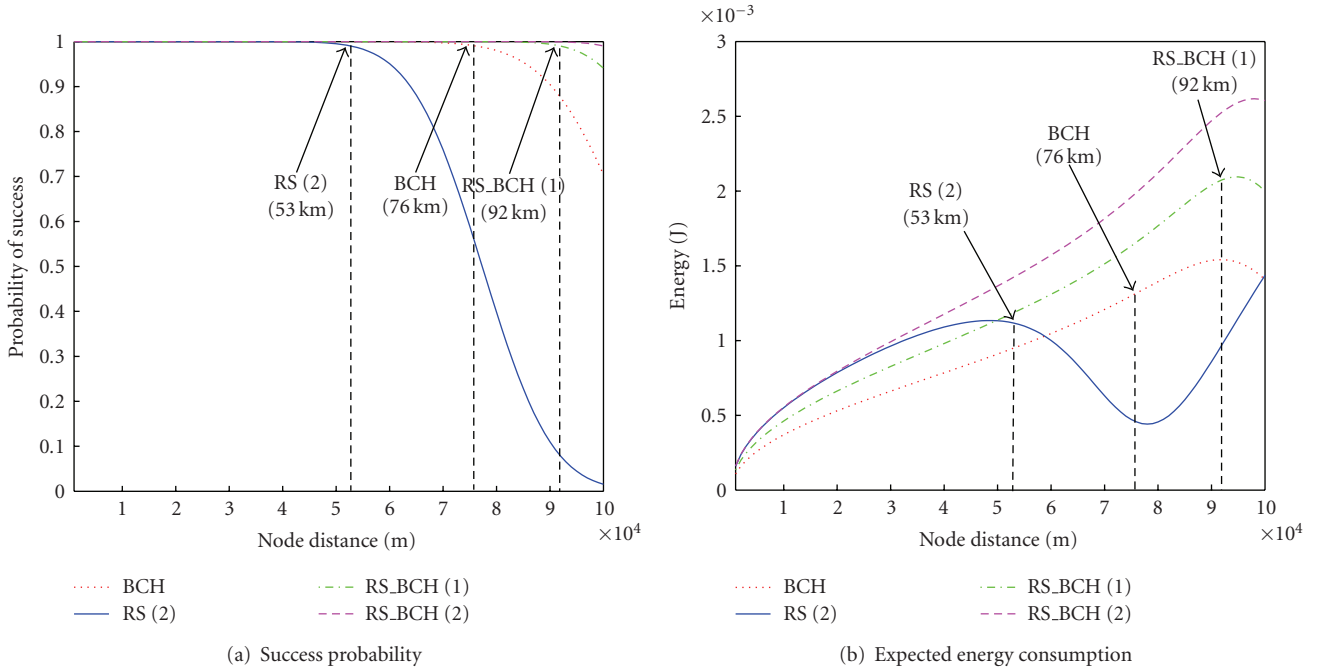
(a) Success probability

(b) Expected energy consumption

Figure 5: Analytical result for the cooperative scenario.

(a) Noncooperative scenario
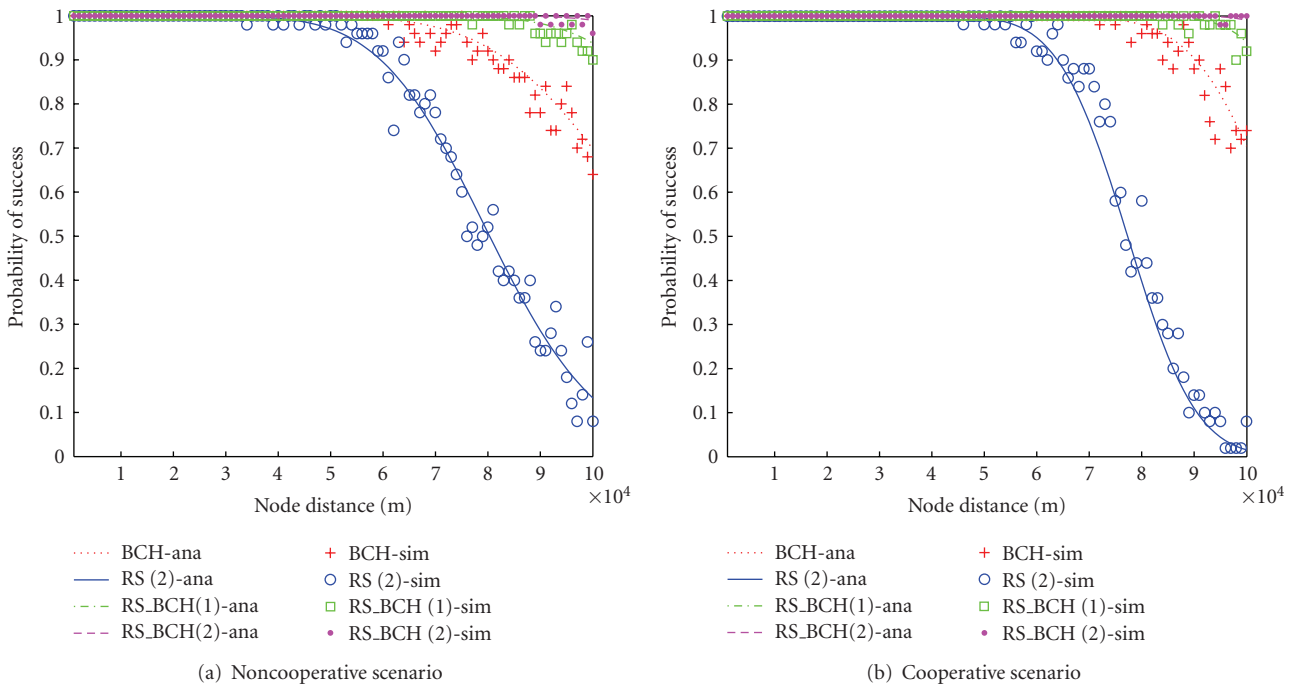
(b) Cooperative scenario

Figure 6: Theoretical and simulated probability of success.

as introduced in Section 3. The signal speed was set to 1500 m/s. In addition, since we mainly focus on the reliable transport issue but not the MAC issue in this paper, a TDMA MAC scheme is employed in the simulations to avoid potential interferences.) We ran 50 simulations and took the average. The results are presented in Figure 6 which confirm the correctness of our theoretical model.

Since the numerical results are credible, we summarize some useful principles obtained from numerical results of Sections 4 and 5.

(i) By considering both the success probability and energy consumption, we should choose different reliable transport schemes (BCH scheme or RS_BCH

scheme) for different internode distance ranges. In addition, the RS scheme should be ignored because it hardly makes a tradeoff between high reliability and low energy consumption.

(ii) To achieve our reliability definition, although some redundant nodes are used, the cooperative communication needs a lower transmission power level and a lower energy consumption. For example, in our numerical results of Figures 3(a) and 5(a), the former needs 131 dB to guarantee reliability within [0.1, 100] km, while this value decreases to 127 dB in the cooperative transmission. Furthermore, in Figures 3(b) and 5(b), BCH, RS_BCH (1), and RS_BCH (2) schemes consume less energy in cooperation than in non-cooperation for the majority of internode distances.

(iii) Compared with noncooperative communication, cooperation can supply additional reliability from the node redundancy for all the schemes. For example, the three thresholds in non-cooperation model are 43 km, 62 km, and 86 km, while they are 53 km, 76 km, and 92 km in cooperation model. For non-cooperation, BCH cannot be used when the node distance is above 62 km, while it is reliable enough until 76 km in the cooperation case. Thus, the scheme thresholds for non-cooperation still hold in the cooperative environment, but, conversely, they do not hold.

6.2. Description of ARRTP. With the above discussions in mind, we propose ARRTP, an adaptive redundancy reliable transport protocol that achieves the best tradeoff between reliability and energy consumption. The protocol is rather simple. For different internode distances, it uses different redundancy schemes.

Let k be the number of data packets in each block transmission and s the maximum possible number of redundancy check packets. Then, from the functions and processing presented in Section 4, we can determine the proper transmission power SL and s distance thresholds θ_1, $\theta_2, \ldots, \theta_s$, where $\theta_0 = 0 < \theta_1 < \theta_2 < \cdots < \theta_s < \theta_{s+1} = d_{\max}$ are the applicable distance boundaries for the BCH, RS_BCH (1), and RS_BCH ($s-1$) schemes. ($d_{\max}$ is the maximum possible internode distance and set to 100 km in this paper.) Based on these thresholds, we can adaptively choose a proper redundancy reliable transport scheme for each interval (θ_i, θ_{i+1}). In other words, for distances shorter than θ_1, ARRTP will use the BCH scheme; between θ_1 and θ_2, RS_BCH (1) scheme is the appropriate candidate, while above θ_s, ARRTP applies RS_BCH (s) scheme. This adaptive configuration can be kept in a *Distance-Strategy Table* by each node.

For example, if k and s are fixed at 4 and 2, there should be two thresholds θ_1 and θ_2 for the BCH scheme and the RS_BCH (1) scheme, and when the internode distance is above θ_2, RS_BCH (2) should be employed. Based on the numerical results of Section 4.3, we can get the appropriate transmission power SL = 131 dB and $\theta_1 = 62$ km, $\theta_2 = $

TABLE 1: DS table for $k = 4$ and $s = 2$.

Distance range (km)	Used scheme
(0, 50]	BCH
(50, 80]	RS_BCH (1)
(80, 100]	RS_BCH (2)

86 km. The *Distance-Strategy Table* for the setting $k = 4$ and $s = 2$ is given in Table 1. Note that in this table we do not absolutely obey the numerical results but reasonably decrease the threshold values to balance the applicable internode distance scopes of each scheme and further increase the reliability.

In ARRTP, the *Distance-Strategy Table (DS Table)* is obtained from the noncooperative scenarios. As we discussed in Section 6.1, the table also holds in the cooperative environment. And when applying the table to cooperative communications, we can reduce the SL to save energy consumption in each node. For example, according to the numerical results of Sections 4 and 5, when using the setting $k = 4$ and $s = 2$, we deploy Table 1 to each node with SL = 131 dB and 127 dB for noncooperative and cooperative next hop transmission, respectively.

Figure 7 describes the implementation framework of ARRTP. When packets need to be sent, the *Scheme Selector and Controller* first chooses which scheme should be used according to the distance to the downstream node and the *DS Table*. The distance is estimated by either a hardware component or an approximate range acquisition algorithm. Note that ARRTP just needs a very rough distance estimation to sustain the *DS Table*, such as Table 1, which costs only a few operations overhead, thus we ignore the energy consumption. Once a data block has reached the data packet queue, depending on the chosen scheme, the data packets will be fed into the RS encoder and then go into the BCH encoder, or bypass the RS encoder and directly enter into the BCH encoder. After finishing the encoding process, finally they will be passed to the MAC layer.

When packets are received, they are first fed into the BCH buffers. After the decoding operation, packets with errors are dropped. If the current node is a cooperative one, it just forwards all the available packets to the destination. And if the receiver is a target node in the routing, then depending on the distance to the downstream node, whether the transmission scheme should be changed is determined. If the transmission scheme needs to be changed according to the *DS table*, then packets are pushed into the data or check packet queues and decoded by the RS decoder. Finally, packets are sent to the upper layer.

7. Simulation

7.1. ARRTP in Two Types of Topology. In this section, we discuss ARRTP in two kinds of topology. We use the same parameter settings as in Sections 4 and 5. And all the results below are averaged from 50 simulations.
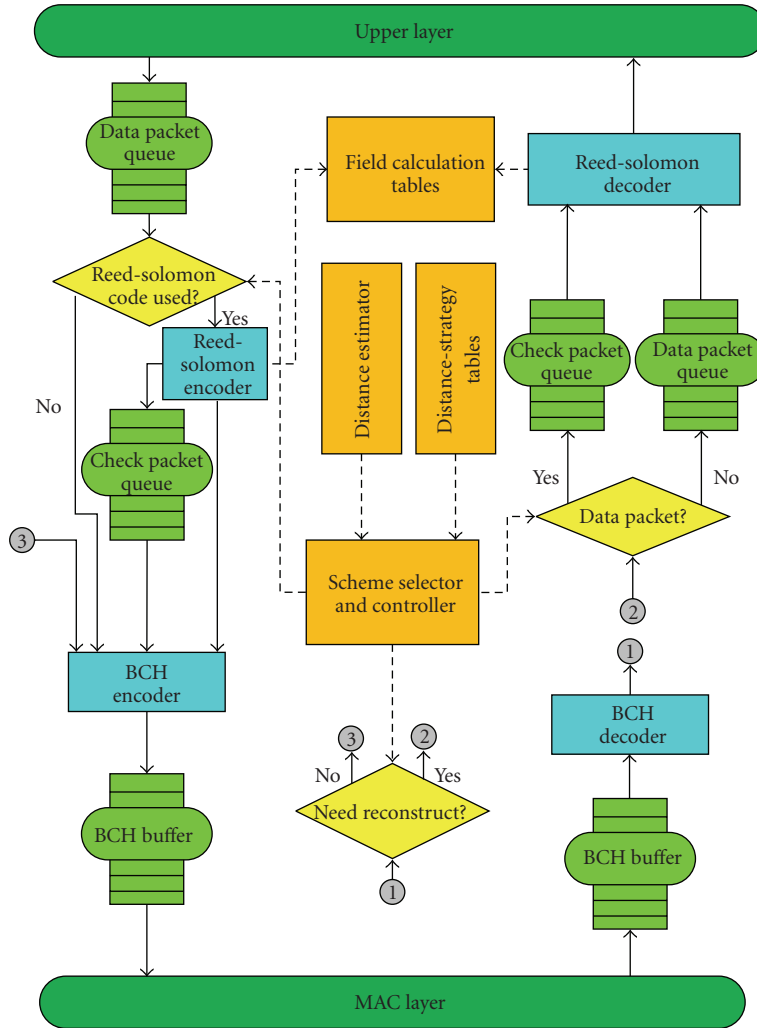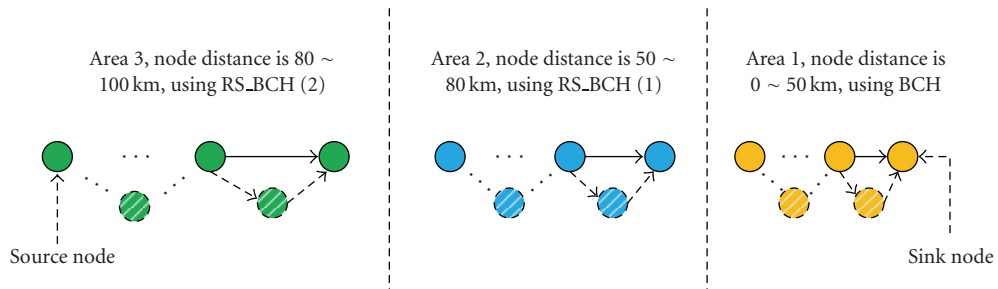
Figure 7: ARRTP implementation framework.

Figure 8: An example of regular topology.

The first type is called *regular topology*. In this case, the whole transmission field is divided into several areas, and hops in each area have similar distances thus nodes use the same schemes in each hop within a certain area according to the *DS Table*. Figure 8 is an example of a *regular topology*. In this example, the data flow comes from the outer area to the sink. There are several hops in one area, and all hops within one area have similar interdistances.

Let $k = 4$ and $s = 2$, the schemes used in each area are chosen according to Table 1. For the simulation of the *regular topology*, we employ the example of Figure 8 and assume that hop distances within an area are equal. We choose 30 km, 60 km, and 90 km as the internode distances in areas 1, 2, and 3 and vary the number of hops inside each area to 1, 3, and 10, respectively. We can clearly see in Figure 9 that ARRTP performs better than the three other

(a) Success probability for the noncooperative case

(b) Energy consumption for the noncooperative case

(c) Success probability for the cooperative case

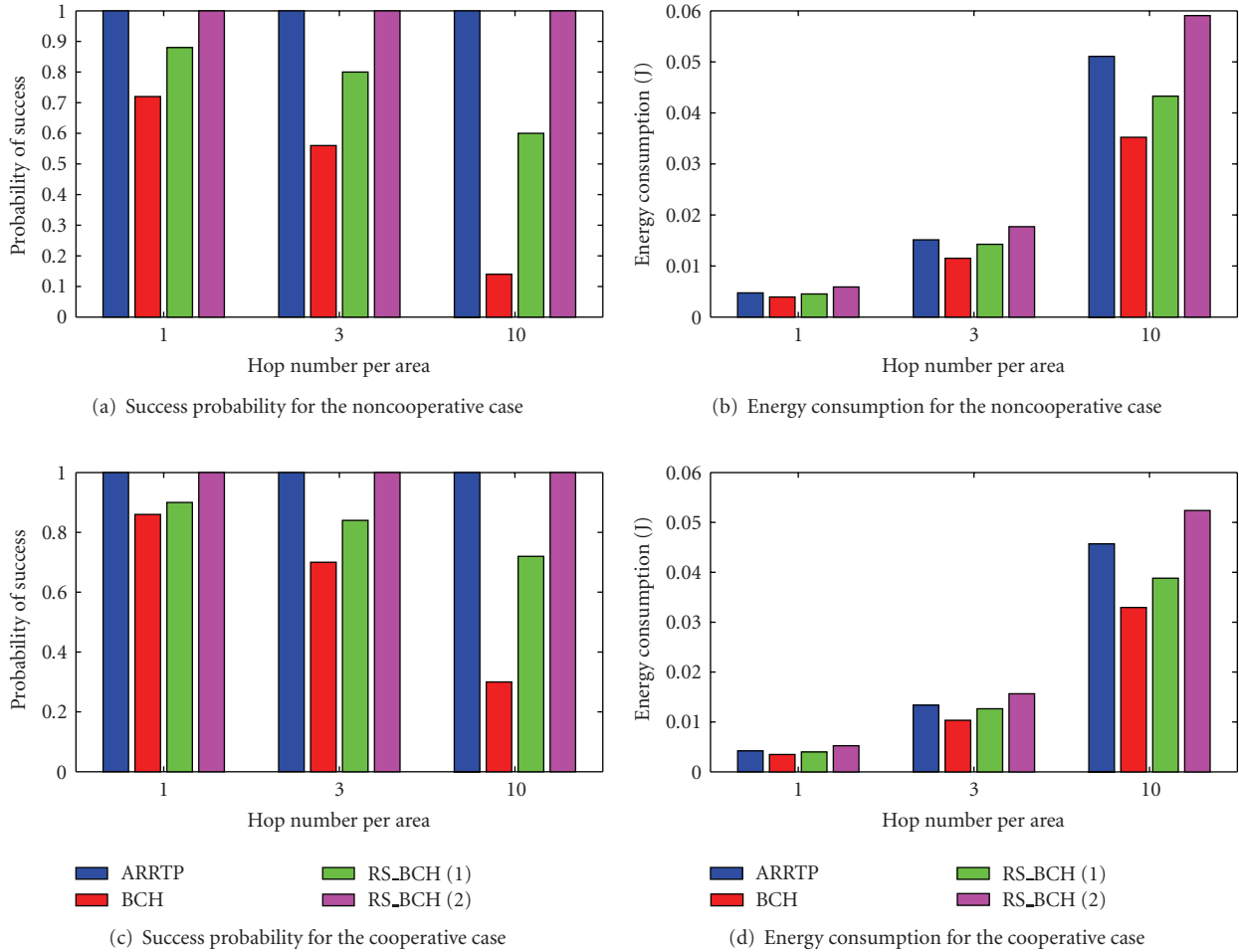(d) Energy consumption for the cooperative case

FIGURE 9: Comparison of the success probability and the energy consumption in the regular topology.

schemes. Both ARRTP and RS_BCH (2) achieve a 100% success probability for transmitting a block of packets in the scenarios with single and multihop communications, but the former consumes less energy. Furthermore, although the cooperative scenario uses a lower source level and consumes less energy, the reliability remains higher than or equal to the noncooperative one. Therefore, the broadcast property of acoustic channels helps save energy.

The second type of topology is more common and is called *random topology*. In a *random topology*, the internode distance of each hop is random. By assuming that the distance of each hop is randomly chosen from $[1, 100]$ km, we set the total hop number to 3, 10, and 30, respectively. The results are similar to the *regular topology* case and given in Figure 10. ARRTP achieves a better tradeoff between the probability of successful transmission and the energy consumption for both scenarios with multihop communication.

7.2. Comparison of the Simulation Results. The simulation results in the previous subsection show that both the ARRTP and RS_BCH (2) schemes bear high transport reliability, while the ARRTP scheme consumes less energy. By defining

the *improvement ratio* (r_{im}), we can calculate the energy savings between ARRTP and RS_BCH (2) from the following formula:

$$r_{\text{im}} = \frac{E_{\text{RS\_BCH}(2)} - E_{\text{ARRTP}}}{E_{\text{RS\_BCH}(2)}} \times 100\%. \qquad (31)$$

For the *regular topology*, the r_{im} for 1, 3, and 10 hops per area that we can get are 19.84%, 14.55%, and 13.52% in a noncooperative scenario, while the values are 19.8%, 14.61%, and 12.77% in cooperative scenario. And in the *random topology*, r_{im} equals 14.68% (3 hops), 20.38% (10 hops), and 23.20% (30 hops) for the noncooperative model and 14.28%, 18.98%, and 18.61% for the cooperative model.

In the *random topology*, the performance of ARRTP depends on the specific distributions of the node distance among hops. For example, when performing the 50 simulations of a noncooperative 30-hop transmission, we noticed that there were 48 simulations in which both RS_BCH (2) and ARRTP successfully transmitted a block of packets passing through 30 hops. Figure 11 depicts the value of r_{im} for these selected cases. We can see that r_{im} varies between 15% and 35%, depending on the topologies.

(a) Success probability for the noncooperative case

(b) Energy consumption for the noncooperative case

(c) Success probability for the cooperative case

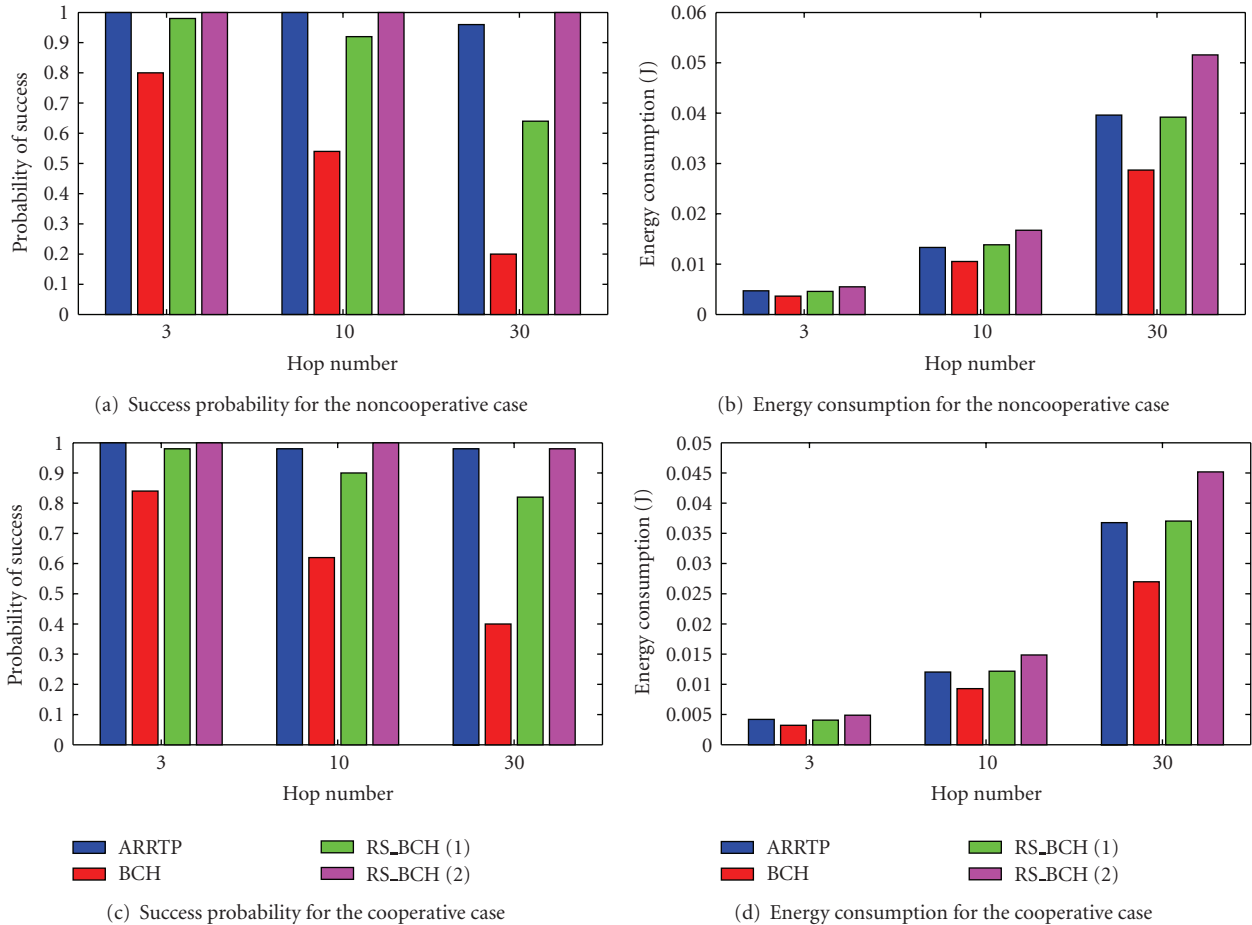(d) Energy consumption for the cooperative case

FIGURE 10: Comparison of the success probability and the energy consumption in the random topology.
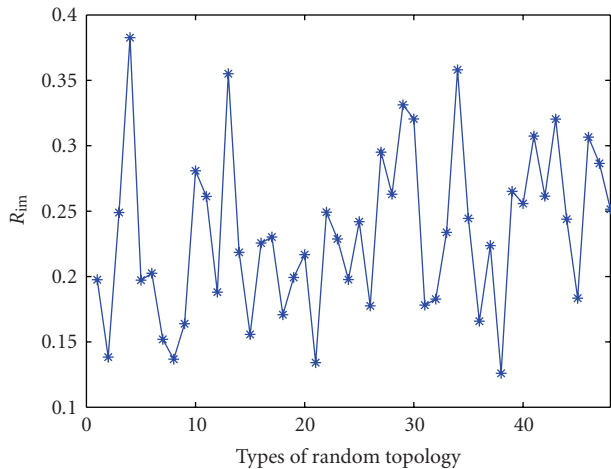

FIGURE 11: R_{im} of 30 hops noncooperative transmission in random topologies.

7.3. ARRTP with Different RS Codes.

In this subsection, we investigate the influences on ARRTP when employing different Reed-Solomon codes. Tables 1, 2, and 3 are the *DS Table* for RS(4, 2), RS(8, 3), and RS(8, 4), respectively,

which can be obtained as described in Section 6.2. (As we use the "look-up table" method to implement RS codes, the table size should be controlled due to the limited storage ability of sensor nodes. Therefore, 4 or 8 packets per block are good choices, but 16 is probably too large, as the look-up table, would require 64 K entries.) We transmit 24 packets passing 30 hops for 10 different distance distribution random topologies in simulations. Thus, the number of required blocks for transmitting the 24 packets is 6, 3, and 3 for RS(4, 2), RS(8, 3), and RS(8, 4), respectively. By the average results in the 10 random topologies of 50 simulations, we calculate the success probability and the average energy consumption of successfully transmitting one packet, which are shown in Figure 12. No matter which kind of RS code is used, ARRTP maintains a very high reliability. We found that a finer division between internode distance and redundancy schemes leads to lower energy consumption; however, it would require more storage space to keep the *Look-up table* for RS codes and cost more processing time for the encoding/decoding operations. For example, according to Tables 1, 2, and 3, RS(4, 2), RS(8, 3), and RS(8, 4) divide the internode distance within (0 km, 100 km] as well as the redundancy schemes into 3, 4, and 5 components, respectively. On the one hand, from Figure 12(b), we can find
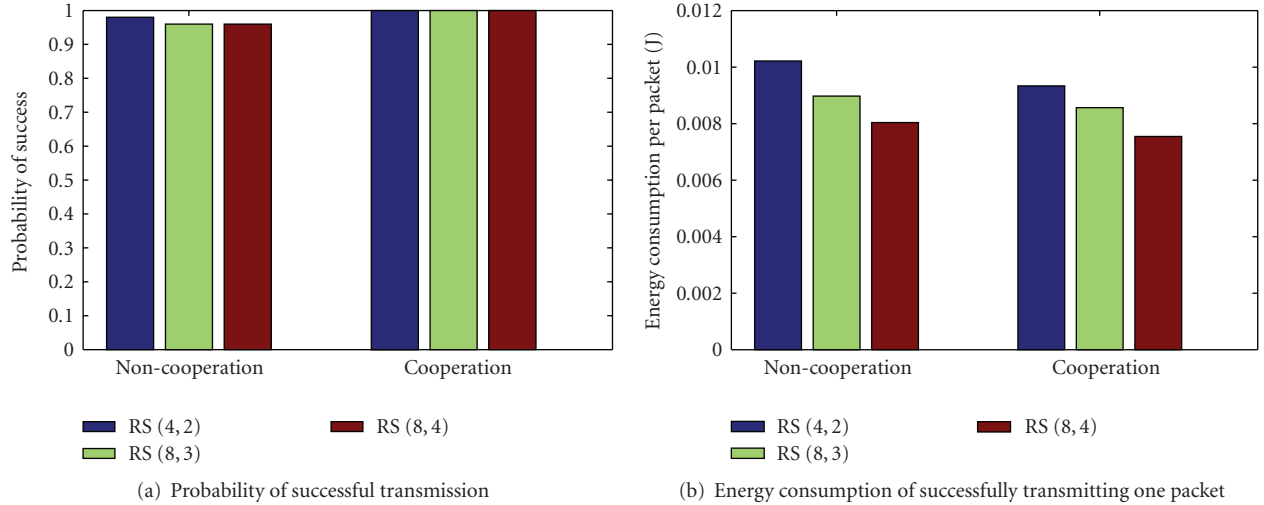
(a) Probability of successful transmission

(b) Energy consumption of successfully transmitting one packet

FIGURE 12: Comparison of success probability and energy consumption in employing different RS codes.

TABLE 2: DS table for $k = 8$ and $s = 3$.

Distance Range (km)	Used Scheme
(0, 45]	BCH
(45, 70]	RS_BCH (1)
(70, 85]	RS_BCH (2)
(85, 100]	RS_BCH (3)

TABLE 3: DS table for $k = 8$ and $s = 4$.

Distance Range (km)	Used Scheme
(0, 40]	BCH
(40, 65]	RS_BCH (1)
(65, 80]	RS_BCH (2)
(80, 90]	RS_BCH (3)
(90, 100]	RS_BCH (4)

that RS(4, 2) with the least components cost the most energy, while RS(8, 4) with the most components cost the least energy. On the other side, compared with RS(4, 2) and RS(8, 3), RS(8, 4) requires more storage space to keep the *Look-up table* and cost more processing time for encoding/decoding operations.

8. Further Discussion

In the previous section, we have discussed some simulations in applying ARRTP to UWSNs; however, ARRTP does not only supply reliability but also has some positive effects on guiding the deployment of underwater sensor nodes. In this section, we offer a simple case to show the initial idea about how to apply ARRTP to topology management. In this case study, a typical topology is used [30]. Figure 13(a) illustrates the generalized network topology. The network

has a multihop centralized topology in which several trees are rooted at the base stations, and data flow is always destined to the base stations which subsequently collect and process the data. We consider the transmit and receive power to be the main sources of power consumption at each node, thus the sensing and processing powers are negligible. Furthermore, we can abstract the topology of Figure 13(a), so that nodes are segmented into tiers as shown in Figure 13(b). The nodes at the lower tier (tier 3 in Figure 13(b)) are the farthest away from the base station and transmit messages to the nodes at the next higher tier (tier 2); tier 1 nodes, which are closest to the base station, finally transmit the data to the base station. For a given path from the lowest tier to the highest tier (tier 1), we consider two specific cases of organization: a linear chain, which applies to environmental monitoring along coastlines, rivers or aqueducts; a grid topology, which applies to other practical environmental monitoring applications such as in a lake or bay.

In the previous work, to investigate different schemes efficiently, we assume that nodes use the distance determinative optimal frequencies, so there may exist several available bit rates in a network which is not very applicable. Hence, here we assume that the bit rates of all the sensor nodes are the same, and set to 2 kHz based on Figure 1(b), which is well within the bit rates of current hydrophones [17]. Then by functions and process in Section 4, we can find an apropos rating source level 133 dB for each sensor node with which Table 1 can be used.

Assuming a batch of sensor nodes deployed to monitor a region of underwater environment, we take the distance between each tier as the varying parameter and propose two distance assignment methods.

(1) Constant intertier distance assignment (CTDA): the intertier distance of each tier is the same. Thus, as we introduced above, a same redundancy scheme can be applied to all the tiers.

(a) A typical topology of UWSNs   (b) A network with three tiers   (c) A grid topology network with 9 nodes
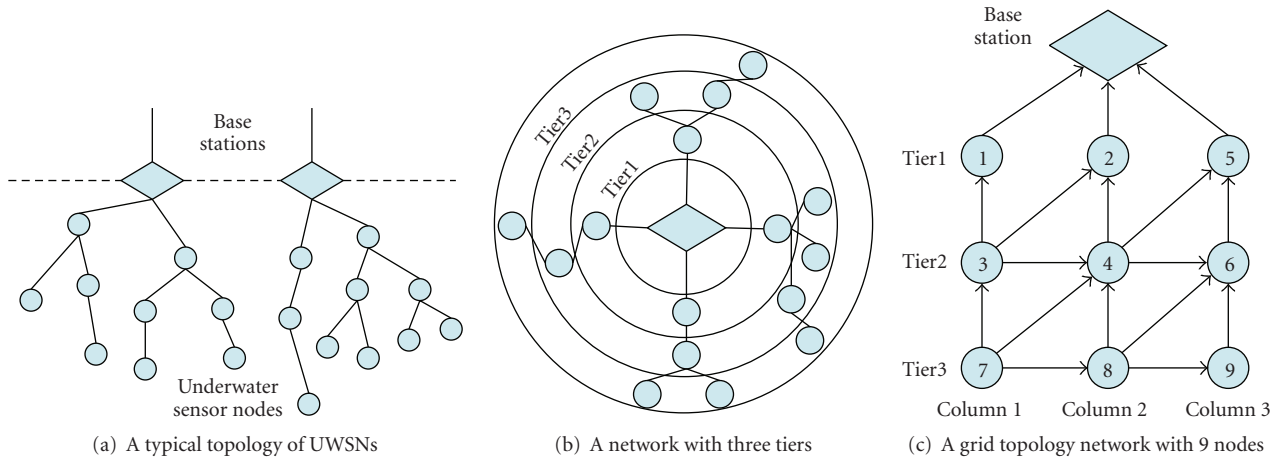
FIGURE 13: The discussed network.

(2) Variable intertier distance assignment (VTDA): (7) and (2) show that distance is the important variable that impacts both SNR and BER. For a certain bit rate and source level, the smaller the internode distance, the lower the BER. Considering that, when compared to the nodes in the higher tiers, nodes in the lower tiers forward more data and play more important roles in the whole network, it would be beneficial to assign distances in a way that reduces the BER of nodes at lower tiers. Similar to the *regular topology*, we divide the tiers into several areas and place the nodes in the lowest area at the shortest intertier distance from the base station, and we increase the intertier distance for each subsequent area. Hence, according to the case of *regular topologies* discussed in Section 7.1, ARRTP becomes the most appropriate redundancy scheme for VTDA.

For CTDA, we use three intertier distances 30 km, 60 km, and 90 km, which we apply to BCH, RS_BCH (1), and RS_BCH (2), respectively. For VTDA, we divide all the tiers into three areas, and each area consists of one third of the tiers. The inter-tier distances and schemes used by ARRTP for the three areas are the same as the three cases of CTDA. Thus, if the network scale (the radius of the lowest tier) is 360 km, we need 12 tiers, 6 tiers and 4 tiers for each CTDA case, but only need a total of 6 tiers, (2 tiers in each of the three areas) for each VTDA case.

We consider a block of packets passing from the lowest tier to the base station; the average of 50 times simulation results is displayed in Figures 14(a) and 14(b). A 100% successful transmission probability is gained by CTDA (30 km/tier), CTDA (60 km/tier), and VTDA. Since a 90 km/tier strategy results in a higher BER than other scenarios, CTDA (90 km/tier) is the only method that supplies a passable reliability. Furthermore, although CTDA (30 km/tier) uses BCH as its redundancy scheme, thus consuming the least energy in one-tier transmission, too many tiers increase the total energy consumption. Therefore, integrating success probability and energy consumption

factors, we conclude that VTDA is an ideal mechanism when deploying underwater sensor nodes.

Figure 13(c) illustrates a representative grid topology of 9 nodes in a UWSN. The node indices indicate the order in which nodes are placed in the grid coverage area [30]. Within the grid topology, nodes self-organize into a triangular lattice, as shown in Figure 13(c). This architecture allows two nodes with the same child to share the load of forwarding the same childs data. Load sharing is beneficial when one of the two parent nodes has fewer children than the other, since the parent nodes can take turns forwarding the common childs data packets. We expect that the distances of the two paths from a child to the two parents to be different, and the biased path to be farther than the beeline path, which means a higher BER and lower reliability. So for the biased path, we use another node to cooperatively transmit the packets.

In the grid topology, the total energy consumption depends on the routing combination from the lowest tier to the highest tier. Since we suppose that all the sensor nodes send signals with the same rating power level (133 dB), the lowest energy consumption is obtained if the beeline paths are used in all the tiers (refer to Figures 14(a) and 14(b)), and the highest one is obtained when biased pathes are used in each tier (refer to Figures 14(c) and 14(d)). If the routing combination is a hybrid of beeline and biased pathes, the energy consumption is between the minimum and the maximum.

However, both the line topology and the grid topology have a similar trend in success probability and total energy consumption, which shows that ARRTP is not only a good transport protocol in UWSNs but also has some positive effect in guiding the deployment of underwater sensor nodes.

9. Conclusion

Due to the singular features of underwater environments, feedback-based protocols like ARQ mechanisms are inconvenient. Therefore, we have naturally focused our work on redundancy solutions. We have studied three schemes that combine redundancy mechanisms at the bit and/or

(a) Success probability in a linear topology

(b) Energy consumption over a linear topology

(c) Success probability in a grid topology

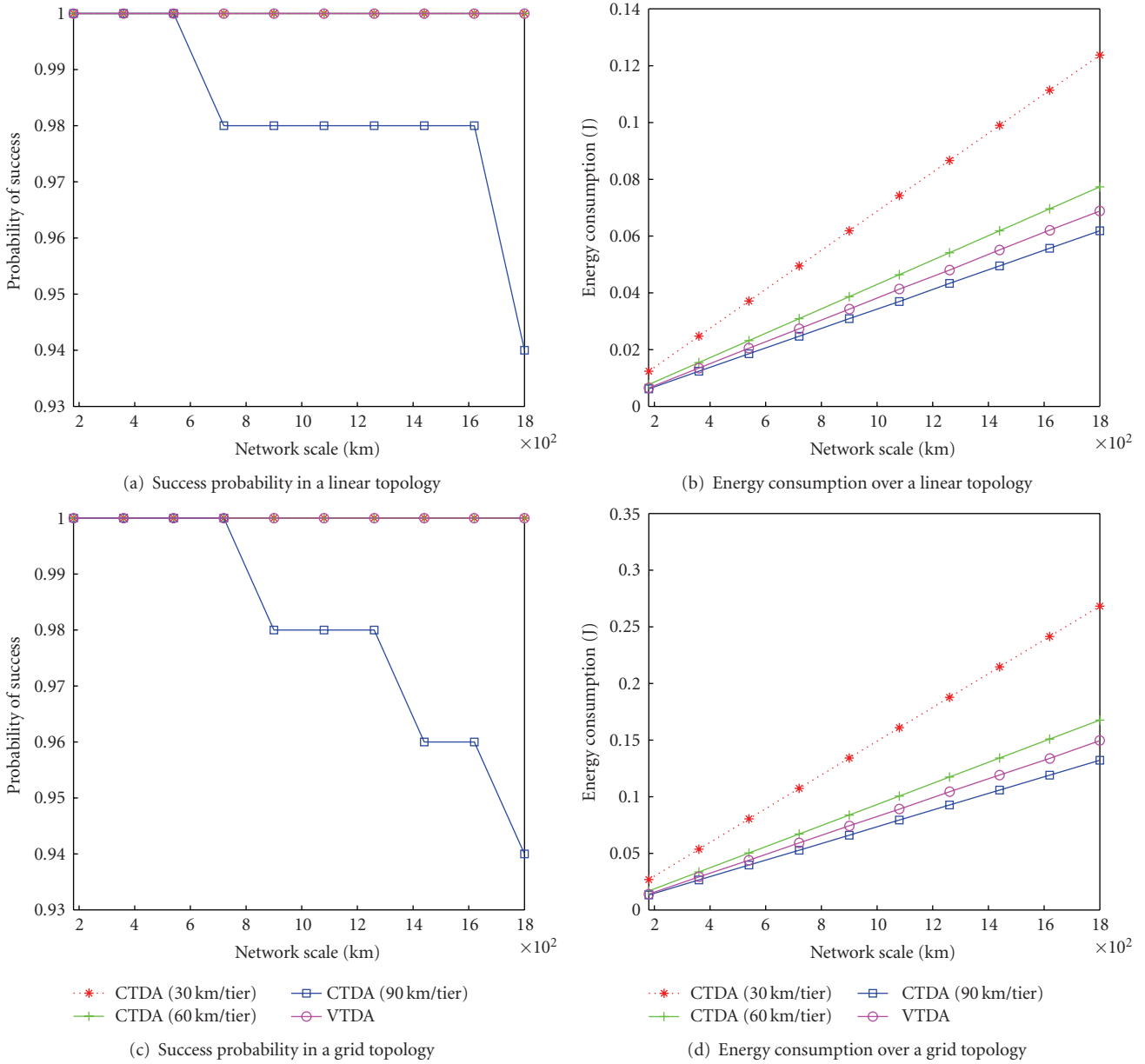(d) Energy consumption over a grid topology

FIGURE 14: Comparison of the success probability and the energy consumption in CTDA and VTDA.

packet level to increase the reliability. Benefitting from the broadcast property of the environment, we have reduced the energy consumption and increased the reliability by using a cooperative approach. The numerical results led us to design an adaptive redundancy transport protocol called ARRTP. Compared with the basic schemes, simulation results demonstrate that this new protocol succeeds in providing a better tradeoff between reliability and energy consumption in both *regular* and *random topologies*. At last, by an integrated case study, we have also shown that besides the merits as a protocol, ARRTP also has some positive effects on guiding the deployment of underwater sensor nodes.

As future work, we would like to further explore the benefits of cooperation in wireless underwater sensor networks. We

intend to compare ARRTP to other bit and packet level redundancy strategies.

Acknowledgment

References

[1] I. F. Akyildiz, D. Pompili, and T. Melodia, "Challenges for efficient communication in underwater acoustic sensor networks," *SIGBED Review*, vol. 1, no. 2, pp. 3–8, 2004.

[2] J. Partan, J. Kurose, and B. N. Levine, "A survey of practical issues in underwater networks," in *Proceedings of the 1st ACM International Workshop on Underwater Networks (WUWNet '06)*, pp. 17–24, Los Angeles, Calif, USA, September 2006.

[3] F. Stann and J. Heidemann, "Rmst: reliable data transport in sensor networks," in *Proceedings of the ACM International Workshop on Wireless Sensor Networks and Applications (WSNA '03)*, pp. 102–112, 2003.

[4] C.-Y. Wan, A. T. Campbell, and L. Krishnamurthy, "PSFQ: a reliable transport protocol for wireless sensor networks," in *Proceedings of the ACM International Workshop on Wireless Sensor Networks and Applications (WSNA '02)*, pp. 1–11, September 2002.

[5] S. Kim, R. Fonseca, and D. Culler, "Reliable transfer on Wireless Sensor Networks," in *Proceedings of the 1st Annual IEEE Communications Society Conference on Sensor and Ad Hoc Communications and Networks (SECON '04)*, pp. 449–459, October 2004.

[6] *IEEE Standard 802. 15. 4 TM*, IEEE Press, New York, NY, USA, 2003.

[7] S. Wicker, *Error Control Coding for Digital Communication and Storage*, Prentice-Hall, Englewood Cliffs, NJ, USA, 1995.

[8] L. Rizzo, "Effective erasure codes for reliable computer communication protocols," *Computer Communication Review*, vol. 27, no. 2, pp. 24–36, 1997.

[9] H.-P. Tan, W. K. G. Seah, and L. Doyle, "A multi-hop ARQ protocol for underwater acoustic networks," in *Proceedings of the IEEE Oceans Conference (OCEANS '07)*, pp. 1–6, June 2007.

[10] P. Xie and J.-H. Cui, "An FEC-based reliable data transport protocol for underwater sensor networks," in *Proceedings of the 16th International Conference on Computer Communications and Networks (ICCCN '07)*, pp. 747–753, August 2007.

[11] H. Medwin, *Sounds in the Sea: From Ocean Acoustics to Acoustical Oceanography*, Cambridge University Press, Cambridge, Mass, USA, 2005.

[12] A. Goldsmith, *Wireless Communications*, Cambridge University Press, Cambridge, Mass, USA, 2005.

[13] R. J. Urick, *Principles of Underwater Sound*, McGraw-Hill, Boston, Mass, USA, 3rd edition, 1983.

[14] W. H. Thorp, "Analytic description of the low-frequency attenuation coefficient," *Journal of Acoustical Society of America*, vol. 42, no. 1, p. 270, 1967.

[15] R. F. Coates, *Underwater Acoustic Systems*, John Wiley & Sons, New York, NY, USA, 1989.

[16] M. Stojanovic, "On the relationship between capacity and distance in an underwater acoustic communication channel," in *Proceedings of the 1st ACM International Workshop on Underwater Networks (WUWNet '06)*, pp. 41–47, Los Angeles, Calif, USA, September 2006.

[17] LinkQuest Inc., "Underwater acoustic modem," 2007.

[18] Y. Sankarasubramaniam, I. F. Akyildiz, and S. W. McLaughlin, "Energy efficiency based packet size optimization in wireless sensor networks," in *Proceedings of the IEEE International Workshop on Sensor Network Protocols and Applications (SNPA '03)*, pp. 1–8, 2003.

[19] A. M. Michelson and A. H. Levesque, *Error-Control Techniques for Digital Communication*, John Wiley & Sons, New York, NY, USA, 1985.

[20] P. Lettieri, C. Schurgers, and M. Srivastava, "Adaptive link layer strategies for energy efficient wireless networking," *Wireless Networks*, vol. 5, no. 5, pp. 339–355, 1999.

[21] Y. Xu, W.-C. Lee, and J. Xu, "Analysis of a loss-resilient proactive data transmission protocol in wireless sensor networks," in *Proceedings of the 1st ACM International Workshop on Underwater Networks (WUWNet '06)*, pp. 17–24, 2006.

[22] M. Luby, "LT codes," in *Proceedings of the 34th Annual Symposium on Foundations of Computer Science (FOCS '02)*, pp. 271–280, November 2002.

[23] D. Barkai, *Peer-to-Peer Computing: Technologies for Sharing and Collaborating on the Net*, Intel Press, 2002.

[24] H. Karvonen, Z. Shelby, and C. Pomalaza-Ráez, "Coding for energy efficient wireless embedded networks," in *Proceedings of the International Workshop on Wireless Ad-Hoc Networks (IWWAN '04)*, pp. 300–304, Oulu, Finland, May-June 2004.

[25] S. Lin and D. J. Costello, *Error Control Coding: Fundamentals and Applications*, Prentice-Hall, Upper Saddle River, NJ, USA, 1983.

[26] M. Goel and N. R. Shanbhag, "Low-power channel coding via dynamic reconfiguration," in *Proceedings of the IEEE International Conference on Acoustics, Speech, and Signal Processing (ICASSP '99)*, pp. 1893–1896, 1999.

[27] Y.-W. Hong, W.-J. Huang, F.-H. Chiu, and C.-C. J. Kuo, "Cooperative communications in resource-constrained wireless networks," *IEEE Signal Processing Magazine*, vol. 24, no. 3, pp. 47–57, 2007.

[28] J. N. Laneman, D. N. C. Tse, and G. W. Wornell, "Cooperative diversity in wireless networks: efficient protocols and outage behavior," *IEEE Transactions on Information Theory*, vol. 50, no. 12, pp. 3062–3080, 2004.

[29] A. F. Harris III and M. Zorzi, "Modeling the underwater acoustic channel in ns2," in *Proceedings of the 2nd International Conference on Performance Evaluation Methodologies and Tools (ValueTools '07)*, October 2007.

[30] S. Phoha, T. F. L. Porta, and C. Griffin, *Sensor Network Operations*, Wiley-IEEE Press, New York, NY, USA, 2006.

[31] L. Bin, F. Garcin, F. Ren, and C. Lin, "A study of forward error correction schemes for reliable transport in underwater sensor networks," in *Proceedings of the 5th Annual IEEE Communications Society Conference on Sensor, Mesh and Ad Hoc Communications and Networks (SECON '08)*, pp. 197–205, 2008.